Metrol. Meas. Syst., Vol. 30 (2023) No. 3, pp. 563–579
DOI: 10.24425/mms.2023.146424

PAN POLSKA AKADEMIA NAUK

METROLOGY AND MEASUREMENT SYSTEMS
Index 330930, ISSN 0860-8229
www.metrology.wat.edu.pl

M&MS

DESIGN OF INSTRUMENTED WHEELSET FOR MEASURING WHEEL-RAIL INTERACTION FORCES

Milan Bižić, Dragan Petrović

University of Kragujevac, Faculty of Mechanical and Civil Engineering in Kraljevo, Dositejeva 19, 36000 Kraljevo, Serbia (✉ *bizic.m@mfkv.kg.ac.rs*, *petrovic.d@mfkv.kg.ac.rs*)

Abstract

The paper presents the design of a specific type of instrumented wheelset intended for continuous measuring of lateral and vertical wheel-rail interaction forces Y and Q, in accordance with regulations EN 14363 and UIC 518. The platform is a standard heavy wheelset BA314 with an axle-load of 25 tons. The key problems of smart instrumentalization are solved by the use of the wheel's numerical FEM model, which provides a significant cost reduction in the initial stage of development of the instrumented wheelset. The main goal is to ensure high measuring accuracy. The results of the FEM calculations in ANSYS are basis for identification of the distribution of strains on the internal and external side of the wheel disc. Consequently, the most convenient radial distances for installation of strain gauges of Wheatstone measuring bridges are determined. In the next stage, the disposition, number and ways of interconnection of strain gauges in the measuring bridges are defined. Ultimately, an algorithm for inverse determination of parameters Y and Q based on mixed signals from the measuring bridges is developed. The developed solution is validated through tests on specific examples, using a created numerical FEM model. A high accuracy of estimation of unknown parameters Y and Q is obtained with an error of less than 4.5%, while the error of estimation of their ratio Y/Q is less than 2%. Therefore, the proposed solution can be efficiently used in the instrumentalization of the considered wheelset, while the problems of its practical implementation will be the subject of further research.

Keywords: instrumented wheelset, wheel-rail interaction forces, derailment coefficient, Y/Q ratio, BA314 wheelset, FEM, ICA.

© 2023 Polish Academy of Sciences. All rights reserved

1. Introduction

Wheel-rail interaction forces Y and Q and their ratio Y/Q are the main indicators of the derailment risk of rail vehicles [1, 2]. International regulations EN 14363 and UIC 518 prescribe the measuring of these forces in most cases of railway vehicle certification processes [3, 4]. Today, such derailment safety tests are mostly performed using instrumented wheelsets that are mounted on the tested wagon. During running, they provide continuous measuring of wheel-rail

Copyright © 2023. The Author(s). This is an open-access article distributed under the terms of the Creative Commons Attribution-NonCommercial-NoDerivatives License (CC BY-NC-ND 4.0 https://creativecommons.org/licenses/by-nc-nd/4.0/), which permits use, distribution, and reproduction in any medium, provided that the article is properly cited, the use is non-commercial, and no modifications or adaptations are made.

Article history: received February 22, 2023; revised April 26, 2023; accepted April 27, 2023; available online September 20, 2023.

interaction forces and derailment coefficient Y/Q of the tested vehicle. The term "continuous" means that the measurement is performed for the entire running time of the tested vehicle, in contrast to stationary wayside systems located at specific points along the railway track where the measurement is performed only at the moments when the tested vehicle passes by it. The mentioned international regulations do not explicate the type, technical solution and necessary measuring accuracy of instrumented wheelsets. Therefore, there are many different approaches and solutions developed in different countries and test centres.

A systematized overview of existing solutions of instrumented wheelsets with their most important characteristics is presented below.

The earliest solutions for instrumented wheelsets appeared in the middle of the last century. In the fifties of the twentieth century, Olson and Jonson proposed a methodology for the indirect measuring of wheel-rail interaction forces based on the measuring of strains of monobloc wheels of an instrumented wheelset [5]. About twenty years later, the methodology of indirect measuring of wheel-rail interaction forces on the basis of measuring of the bending moments of the axle of an instrumented wheelset was developed [6, 7]. The approach of measuring of wheel-rail interaction forces over wheels had proved much better and further development of instrumented wheelsets was proceeding in the same direction. At the end of the last century, British Railways developed, at the time superior, instrumented wheelsets with spoked wheels [8]. Despite the different directions of development and approaches, instrumented wheelsets composed of typical monobloc wheels are most often used today. In this way, standard wheelsets can be used for the production of instrumented wheelsets, without any subsequent machining. However, modern solutions vary as it comes to the locations for installation of strain gauges, their disposition and interconnection method, signal transmission and processing, calibration method, method of inverse determination of measured parameters, *etc.*

Bracciali *et al.* [9] studied existing technologies of development of instrumented wheelsets with applications and gave their systematized review, while basic problems were analysed by Bižić and Petrović [10]. The method of calibrating the dynamometer, *i.e.*, an instrumented wheelset for measuring the wheel-rail interaction forces was studied by Diana *et al.* in [11]. Gialleonardo *et al.* [12] and Bracciali *et al.* [13] proposed new solutions for test stands for the calibration of instrumented wheelsets. Gialleonardo *et al.* [14] presented a methodology for calibrating the instrumented wheelsets using the model in order to significantly reduce time and costs. The problems of testing the calibration and correction of the instrumented wheelset were analysed in [15] by Lin *et al.*, Jin *et al.* [16] presented a new approach in the calibration process with the goal to obtain a higher signal-to-noise ratio and improve measuring accuracy of instrumented wheelsets.

Bagheri *et al.* [17] and Papini *et al.* [18] investigated techniques for optimal placement of strain gauges and precise design of instrumented wheelsets in order to minimize the effects of various disturbance factors such as wheel rotation, temperature, centrifugal acceleration, noise, *etc.*

Various solutions for improvement the signal quality and measuring accuracy of instrumented wheelsets were proposed in [19] by Gomez *et al*. Cazzulani *et al.* [20] proposed a new method for increasing the measuring accuracy in the case when a high derailment coefficient Y/Q is reached. With the aim of improving the quality of continuous measuring of the wheel-rail interaction forces with instrumented wheelsets, a new approach based on state space theory was presented in [21] by Ren *et al.*

The method of measuring the position of the interaction point among the wheel and rail was studied by Kanehara and Fujioka in [22], Hondo *et al.* in [23] and Noguchi in [24]. Methods of improvement of measuring the lateral force in wheel-rail interaction using instrumented wheelsets were investigated in [25] and [26] by Hondo *et al.* In [27] Hondo *et al*. studied the possibility of

Metrol. Meas. Syst., Vol. 30 (2023), No. 3, pp. 563–579
DOI: 10.24425/mms.2023.146424

increasing the measuring accuracy of instrumented wheelsets, taking into account the effects of longitudinal force and lateral change of the wheel-rail interaction point.

Wei *et al*. [28] proposed a method for measuring the wheel-rail interaction forces using an instrumented wheelset and axle-boxes, while Urda *et al.* [29] presented an approach using strain gauges on the instrumented wheelset and distance lasers for measuring the wheel disc deflections. Problems of signal transmission and power supply for instrumented wheelsets were studied by Wand *et al.* [30] and Hanbiao *et al.* [31]. Ronasi *et al.* [32] studied the problem of determination the wheel-rail interaction forces based on the measured strains when the interaction forces are determined by minimizing the least-squares discrepancy between the measured radial strains and corresponding computed strains from a three-dimensional finite-element model of the wheel.

The main goal of all presented research is to provide opportunities for increasing the measuring accuracy of instrumented wheelsets. For this purpose, one of the most important aims is finding the most convenient way for inverse determination of the measured parameters, *i.e.*, for the separation of mixed signals, which is subject of a very limited number of studies and publications. One of the most powerful approaches in developing modern instrumented wheelsets is the usage of *blind signal separation* (BSS) methods, as presented by Ren *et al.* in [33] and [34]. In addition, BSS and *independent component analysis* (ICA) were efficiently used by the authors of this paper in developing a method of measuring the wheel-rail interaction forces and position of the interaction point, which is presented in [35] and [36].

Accordingly, the aim of this paper is to present the design of a specific type of instrumented wheelset on the platform of a standard heavy BA314 wheelset with an axle-load of 25 tons. It is intended for continuous measurement of lateral and vertical forces Y and Q in the wheel-rail interaction, *i.e.*, the derailment coefficient Y/Q, in accordance with international regulations EN 14363 and UIC 518. The presented approach ensures considerable lowering in the costs of developing instrumented wheelsets, given that the most important problems are solved using the numerical FEM model of the wheel.

2. Radial distances for strain gauge installation

The platform for development of the instrumented wheelset is a standard wheelset BA314 for heavy freight wagons with an axle-load of 25 tons. The wheelset mass is 1046 kg and it is designed for a maximum speed of 120 km/h. The nominal mass of the wheel is 330 kg, while its material is ER7 in accordance with EN 13262 [37]. The wheel's numerical FEM model is formed in ANSYS software and contains 371666 nodes and 238978 finite elements of the tetrahedron type. The stress-strain analysis of the wheel is performed using the *finite element method* (FEM) for six representative load-cases, as presented in Fig. 1.

The selected load-cases take into account typical locations of the interaction point such as nominal contact CP-1, contact near the external side of the wheel CP-2 and flange contact CP-3.

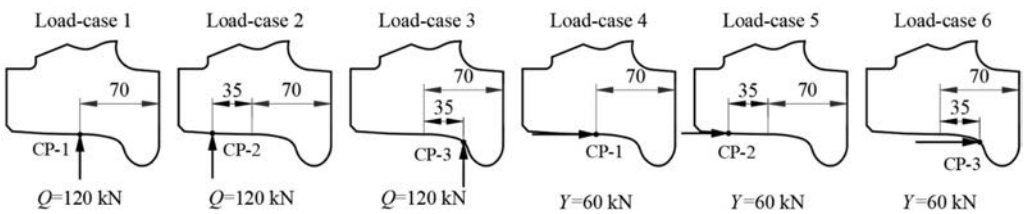

Fig. 1. Representative load-cases for stress-strain analysis of the wheel.

Based on the results of FEM calculation for the given load-cases, diagrams of radial strains on the internal and external sides of the wheel disc are formed in the section above the interaction point. Two examples of results of calculations for radial strains in ANSYS are presented in Figs. 2 and 3, while diagrams of radial strain distribution are presented in Figs. 4–7. These diagrams are grouped and presented in a way which ensures that the characteristics of the wheel disc under the action of lateral and vertical forces are more intuitive and suitable for further analysis.

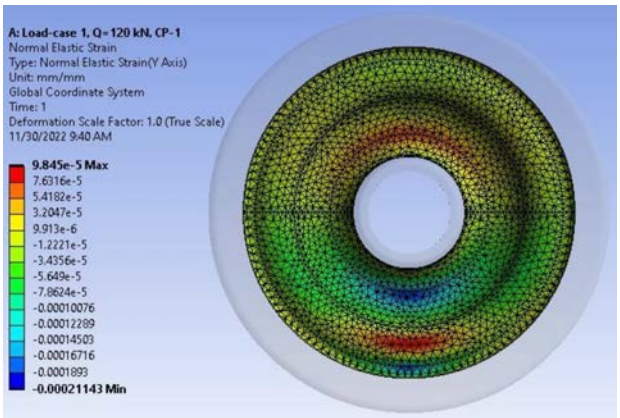

Fig. 2. Results of calculation of radial strain on the internal disc side for Load-case 1 (Q = 120 kN, CP-1).

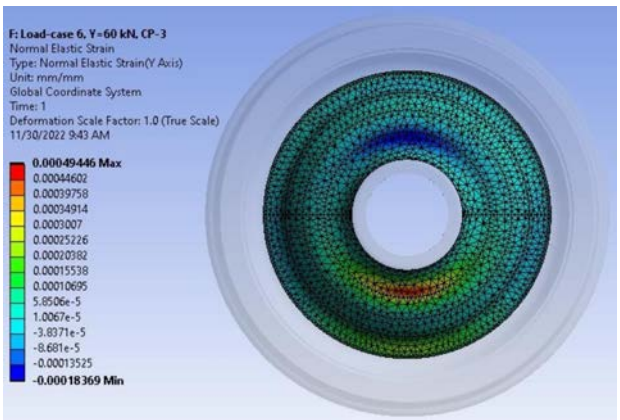

Fig. 3. Results of calculation of radial strain on the external disc side for Load-case 6 (Y = 60 kN, CP-3).

The obtained results showed that the change of position of lateral force Y has no effect on the radial strains of the wheel disc (see diagrams in Figs. 6 and 7). Therefore, the most convenient radial distance for installation of the strain gauges of the measuring bridge for measurement of force Y is the distance with the highest value of strain. It is located on the external side of the wheel disc, at a distance of 186 mm from the centre of the wheel (see diagram in Fig. 7). At this radial distance, the differences in strain values for the analysed load-cases are below 2%.

Metrol. Meas. Syst., Vol. 30 (2023), No. 3, pp. 563–579
DOI: 10.24425/mms.2023.146424

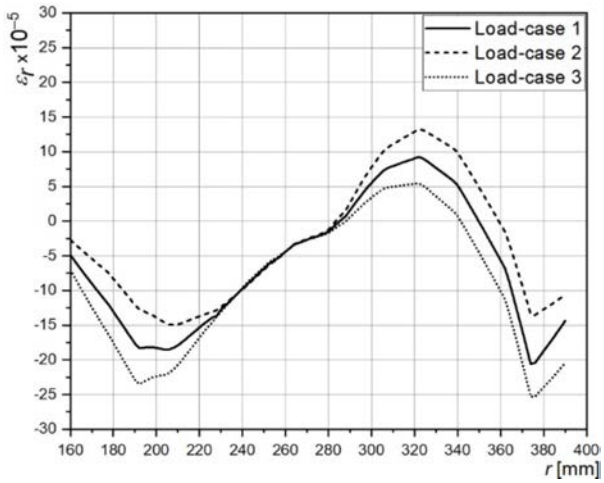

Fig. 4. Distribution of radial strains on the internal side of the wheel disc under the action of force Q (Load-cases 1, 2 and 3).

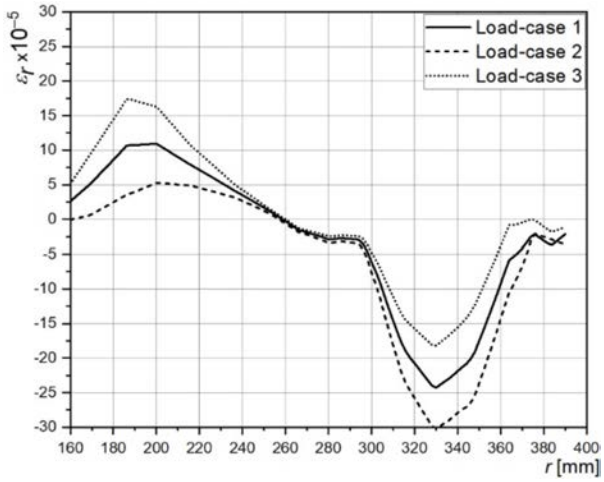

Fig. 5. Distribution of radial strains on the external side of the wheel disc under the action of force Q (Load-cases 1, 2 and 3).

Therefore, placing strain gauges at this radial distance will ensure that the output signals from the measuring bridge are insensitive to changing the location of application of force Y.

Further, the results showed that change of point of application of vertical force Q has an effect on the radial strains of the wheel disc (see diagrams in Figs. 4 and 5). There is only one radial distance where the strain values for the analysed load-cases are very close and it is located on the internal side of the disc at a distance of 236 mm from the wheel centre (see diagram in Fig. 4). At this radial distance, on the internal side of the wheel disc, the strain values for analysed Load-cases 1, 2 and 3 are $\varepsilon_{r1} = -10.98 \cdot 10^{-5}$, $\varepsilon_{r2} = -10.89 \cdot 10^{-5}$ and $\varepsilon_{r3} = -11 \cdot 10^{-5}$, respectively. The differences in the strain values for given load-cases are below 1%, so this radial

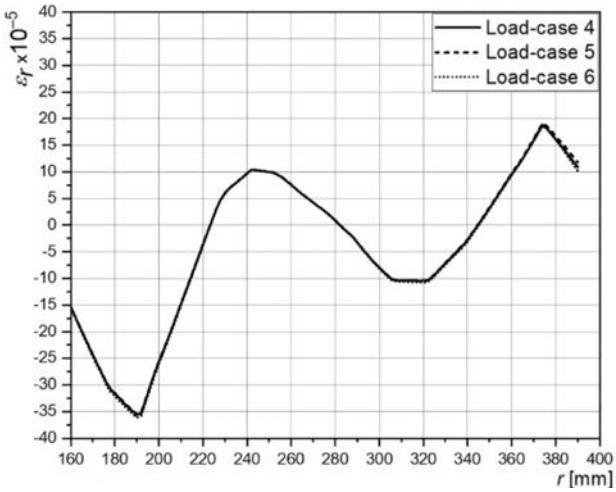

Fig. 6. Distribution of radial strains on the internal side of the wheel disc under the action of force Y (Load-cases 4, 5 and 6).

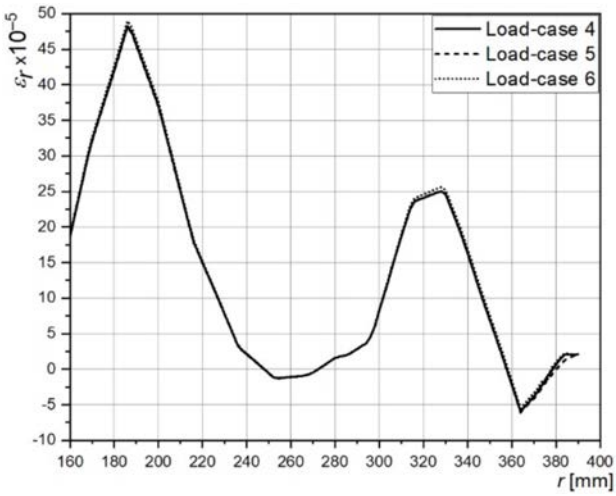

Fig. 7. Distribution of radial strains on the external side of the wheel disc under the action of force Y (Load-cases 4, 5 and 6).

distance is the most convenient for installing of strain gauges of bridge for measuring force Q. In this way, it is ensured that the output signals from this measuring bridge are insensitive to changing the location of application of force Q.

Ultimately, the selected radial distances for installation of the strain gauges of measuring bridges for forces$Y$ and Q measuring are presented in Fig. 8.

Therefore, the core of this approach is that it ensures the neutralization of the influence of contact point position change on the output signals from the measuring bridges, that is, on the measurement of wheel-rail interaction forces.

Metrol. Meas. Syst., Vol. 30 (2023), No. 3, pp. 563–579
DOI: 10.24425/mms.2023.146424

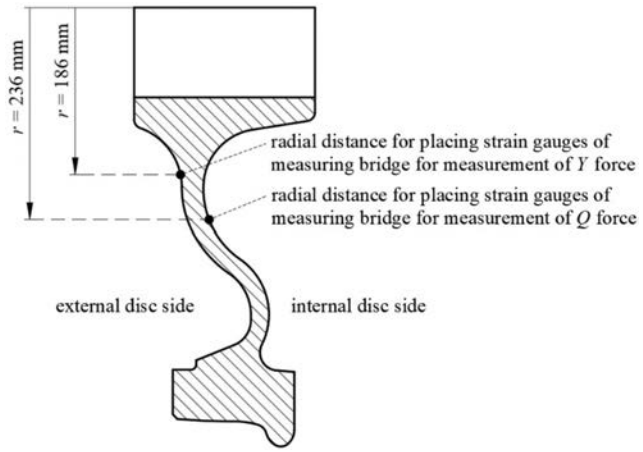

Fig. 8. Selected radial distances for installing the strain gauges of measuring bridges for measuring forces Y and Q.

3. Disposition and interconnection of strain gauges

The disposition of the strain gauges at determined radial distances is given in Fig. 9, while the way of their interconnecting into the Wheatstone measuring bridges is presented in Fig. 10. Four strain gauges at each radial distance are interconnected in a full-bridge configuration. The signal from such a measuring bridge changes depending of the speed of movement and the angular placement of the instrumented wheel. The maximum values of the signal are obtained at the moments when each of the strain gauges passes above the interaction point. Therefore, for one rotation of the wheel, there are four representative signal values that should be entered into the algorithm for inverse determination of the parameter being measured. The appearance of measurement signals obtained from the measuring bridges during one wheel revolution and discrete values relevant for the determination of unknown parameters in the wheel-rail interaction are shown in Fig. 11.

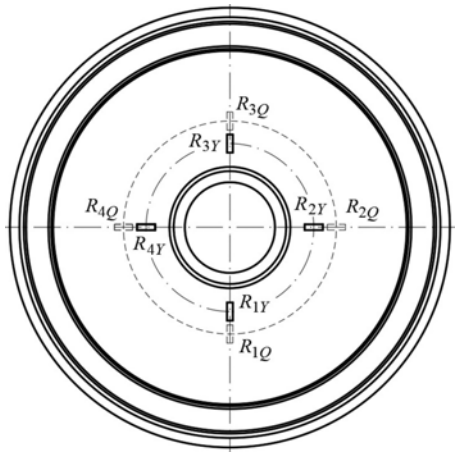

Fig. 9. Disposition of strain gauges at determined radial distances.

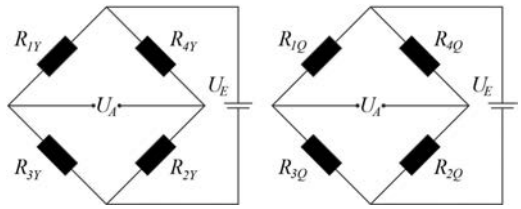

Fig. 10. Way of interconnection of strain gauges in the measuring bridges.

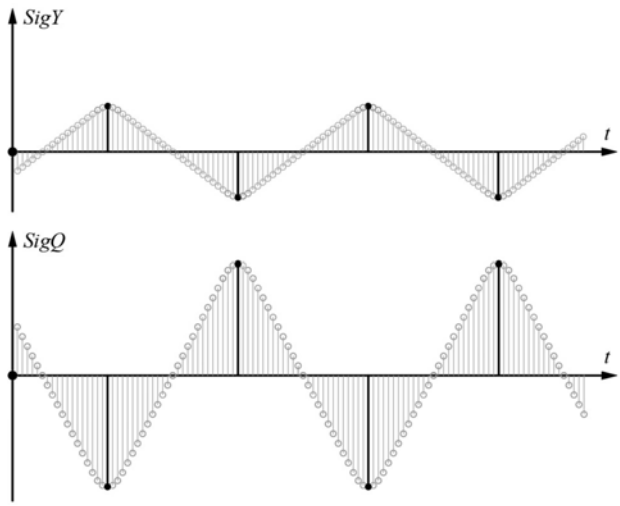

Fig. 11. Appearance of measurement signals obtained from the measuring bridges during one wheel revolution and discrete values relevant for the determination of unknown parameters in the wheel-rail interaction.

The way of interconnecting the strain gauges shown in Fig. 10 is selected with the aim of obtaining the highest possible values of output signals from the measuring bridges. This is performed on the basis of the created wheel's numerical FEM model and calculation of the strains at the strain gauge positions. It is significant to emphasize that the defined interconnection method provides compensation of the impacts of temperature, centrifugal acceleration and other parasitic effects during running.

The output signals from the measuring bridges (Figs. 9–10) whose appearance is shown in Fig. 11 are defined by the following equations:

$$SigY = \left(\frac{U_A}{U_E}\right)_Y = \frac{k_{sg}}{4} \cdot (\varepsilon_{1Y} + \varepsilon_{2Y} - \varepsilon_{3Y} - \varepsilon_{4Y}), \tag{1}$$

$$SigQ = \left(\frac{U_A}{U_E}\right)_Q = \frac{k_{sg}}{4} \cdot (\varepsilon_{1Q} + \varepsilon_{2Q} - \varepsilon_{3Q} - \varepsilon_{4Q}), \tag{2}$$

where: k_{sg} – factor of strain gauges known as the "gauge factor", ε_{1Y}, ε_{2Y}, ε_{3Y}, ε_{4Y} – strain values registered by the strain gauges measuring electrical resistances R_{1Y}, R_{2Y}, R_{3Y} and R_{4Y} on the bridge for measuring force Y, ε_{1Q}, ε_{2Q}, ε_{3Q}, ε_{4Q} – strain values registered by strain gauges measuring electrical resistances R_{1Q}, R_{2Q}, R_{3Q} and R_{4Q} on the bridge for measuring force Q.

The previous equations (1) and (2) allow to calculate the values of the output mixed signals from the measuring bridges for specific load cases, on the basis on the strain values obtained with the numerical FEM model.

A particular problem for the practical implementation of the presented concept is extracting the values of the signal at the instants at which the strain gauges pass above the interaction point (see Fig. 11). This requires a special processing unit and appropriate sensors with the wheel's angular placement [36]. However, this is outside the scope of this research and will be included in further research, which will be related to solving the problems of practical implementation of the presented solution.

4. Algorithm for inverse determination of measured parameters Y and Q

The main task of the inverse determination algorithm is to ensure the estimation of source single values of the unknown parameters Y and Q, on the basis of mixed signals (see Fig. 11) from the measuring bridges as shown in Figs. 9 and 10.

The signal mixing procedure is schematically presented in Fig. 12, while the signal separation procedure is presented in Fig. 13. The simultaneous effect of the original unknown parameters Y and Q at the movement of the instrumented wheelset in time (t) causes mixed output signals from measuring bridges $SigY$ and $SigQ$ (see Fig. 12). These output signals should be introduced into the algorithm for blind signal separation $i.e.$, inverse determination of the parameters being measured. As a result of the separation procedure, the estimated values of the measured parameters Y_e and Q_e are obtained (see Fig. 13).

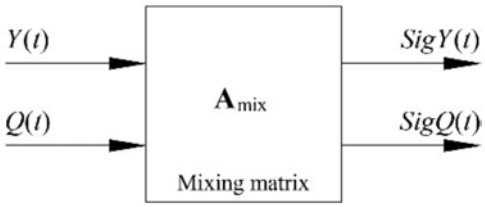

Fig. 12. Signal mixing procedure.

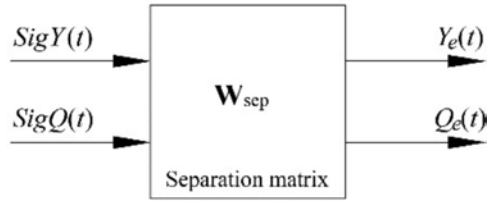

Fig. 13. Signal separation procedure.

The procedure of signals mixing shown in Fig. 12 can be mathematically formulated as follows:

$$\mathbf{S}_{\text{exit}}(t) = \mathbf{A}_{\text{mix}} \cdot \mathbf{S}_{\text{orig}}(t), \tag{3}$$

where: $\mathbf{S}_{\text{exit}}(t)$ – vector of output mixed signals from two measuring bridges that has the following form:

$$\mathbf{S}_{\text{exit}}(t) = \begin{Bmatrix} SigY(t) \\ SigQ(t) \end{Bmatrix}, \tag{4}$$

$\mathbf{A}_{\text{mix}}$ – square matrix of mixing which is unknown and has the following form:

$$\mathbf{A}_{\text{mix}} = \begin{bmatrix} a_{11} & a_{12} \\ a_{21} & a_{22} \end{bmatrix}, \tag{5}$$

$\mathbf{S}_{\text{orig}}(t)$ – vector of original signals of parameters Y and Q being measured that has the following form:

$$\mathbf{S}_{\text{orig}}(t) = \begin{Bmatrix} Y(t) \\ Q(t) \end{Bmatrix}. \tag{6}$$

Additionally, the procedure of signal separation shown in Fig. 13 can be formulated as follows:

$$\mathbf{S}_{\text{est}}(t) = \mathbf{W}_{\text{sep}} \cdot \mathbf{S}_{\text{exit}}(t), \tag{7}$$

where: $\mathbf{S}_{\text{est}}(t)$ – vector of estimated signals of parameters being measured that has the following form:

$$\mathbf{S}_{\text{est}}(t) = \begin{Bmatrix} Y_e(t) \\ Q_e(t) \end{Bmatrix}, \tag{8}$$

$\mathbf{W}_{\text{sep}}$ – square separation matrix which is also unknown and can be determined as an inverse matrix of the mixing matrix, *i.e.*:

$$\mathbf{W}_{\text{sep}} = \mathbf{A}_{\text{mix}}^{-1} = \begin{bmatrix} a_{11} & a_{12} \\ a_{21} & a_{22} \end{bmatrix}^{-1}. \tag{9}$$

The determination of the unknown square matrix of separation $\mathbf{W}_{\text{sep}}$ is performed over the calibration of the measuring system.

Thus, during one wheel revolution, the four maximum discrete values of each of the two measuring signals are introduced into the presented inverse determination algorithm. By solving the problem of inverse determination, the estimated signals of the measured parameters Y and Q are obtained (Fig. 14). These signals represent discrete values whose intensity changes during running.

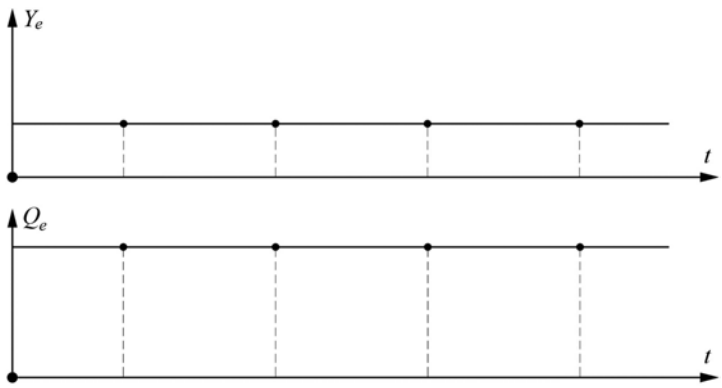

Fig. 14. Appearance of the estimated signals of the measured parameters Y and Q as a result of solving the problem of inverse determination.

4.1. Calibration process

At this stage of designing of the instrumented wheelset, calibration is performed on the basis of the created numerical FEM model of the wheel. In the practical implementation of the developed concept, which will be the subject of further research, the problem of calibration of a real object should be solved using a special test rig, as presented in [36]. In both cases, based on the outcomes of the calibration process, the unknown separation matrix $\mathbf{W}_{\text{sep}}$ is determined based on the expression:

$$\mathbf{W}_{\text{sep}} = \mathbf{S}_{\text{cal}} \cdot \mathbf{S}_{\text{exit,cal}}^{-1}, \tag{10}$$

where: $\mathbf{S}_{\text{cal}}$ – matrix of concrete values of parameters Y and Q which are set during the calibration process using the numerical FEM model (or using a test rig), $\mathbf{S}_{\text{exit,cal}}$ – matrix of registered signals

from the measuring bridges under the action of specified parameters Y and Q in the calibration process.

The calibration process and determining the matrices $\mathbf{S}_{\text{cal}}$ and $\mathbf{S}_{\text{exit,cal}}$ should be based on typical and representative load-cases which cover the most common situations in the wheel-rail interaction, as shown in Fig. 15. In the case of a slightly different choice of contact points and parameter values, practically the same separation matrix will be obtained with minor and negligible deviations.

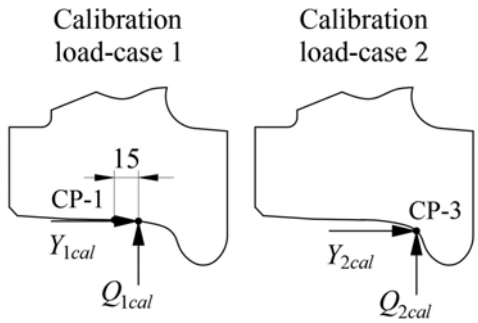

Fig. 15. Representative load-cases for the calibration process.

Therefore, for efficient calibration, only two different measurements need to be performed, as shown in Fig. 15, while the unknown matrices have the following forms:

$$\mathbf{S}_{\text{cal}} = \begin{bmatrix} Y_{1\text{cal}} & Y_{2\text{cal}} \\ Q_{1\text{cal}} & Q_{2\text{cal}} \end{bmatrix}, \tag{11}$$

$$\mathbf{S}_{\text{exit,cal}} = \begin{bmatrix} SigY_{1\text{cal}} & SigY_{2\text{cal}} \\ SigQ_{1\text{cal}} & SigQ_{2\text{cal}} \end{bmatrix}. \tag{12}$$

In the first load case – calibration measurement, parameters $Y_{1\text{cal}}$ and $Q_{1\text{cal}}$ act simultaneously and produce signals in the measuring bridges $SigY_{1\text{cal}}$ and $SigQ_{1\text{cal}}$, while in the second one parameters $Y_{2\text{cal}}$ and $Q_{2\text{cal}}$ act simultaneously and produce signals $SigY_{2\text{cal}}$ and $SigQ_{2\text{cal}}$.

5. Validation of the developed solution

The task of this chapter is to test the effectiveness of the developed solution on several specific examples. For this purpose, the wheel's numerical FEM model is again used.

In the first stage, calibration is realized using the numerical FEM model, according to the procedure described in Section 4.1. The values of the calibration parameters shown in Fig. 15 are given in Table 1.

Table 1. Values of parameters for calibration.

	Load-case 1	**Load-case 2**
Y_{cal} [kN]	15	60
Q_{cal} [kN]	120	135

Therefore, matrix (11) has the following form:

$$\mathbf{S}_{\text{cal}} = \begin{bmatrix} 15 & 60 \\ 120 & 135 \end{bmatrix}. \tag{13}$$

For these values of the calibration parameters, the following matrix (12) is obtained based on the strain values from the numerical FEM model and expressions (1) and (2):

$$\mathbf{S}_{\text{exit,cal}} = \begin{bmatrix} 190.1426 & 495.7720 \\ -52.7117 & -29.2668 \end{bmatrix}. \tag{14}$$

The values of the gauge factor $k_{sg} = 2.05$ are used and the strain values are expressed in [μdef], so the signal values in matrix (14) are obtained in units [mV/V]. For matrices (13) and (14) constructed in this way, the next matrix of separation is obtained:

$$\mathbf{W}_{\text{sep}} = \begin{bmatrix} 0.132423 & 0.193113 \\ 0.175226 & -1.644460 \end{bmatrix}. \tag{15}$$

Matrix (15) is used in testing the developed concept in five specific test cases that are shown in Fig. 16. The displayed loads Y and Q, *i.e.* the ratio Y/Q, in each test-case are simultaneously set in the numerical FEM model and the output mixed signals from the measuring bridges are calculated based on the obtained strain values and expressions (1) and (2). These mixed signals are entered into the inverse determination algorithm, *i.e.*, they are multiplied by the separation matrix (15) and thus the original signals of values of the parameters Y and Q set in the numerical FEM model are estimated.

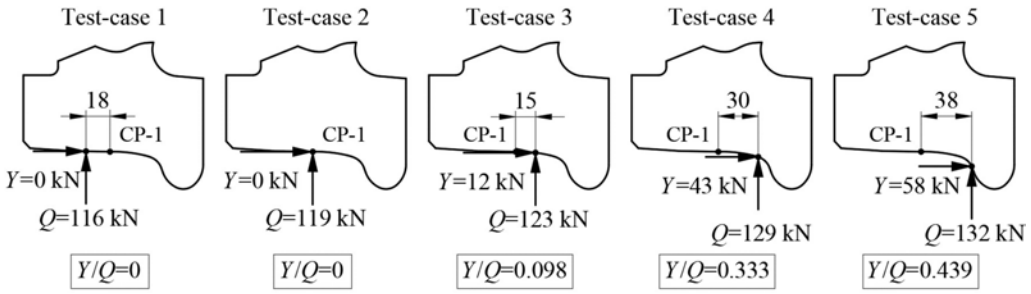

Fig. 16. Specific cases for testing the developed solution.

For the given Test cases 1–5, the following mixed signals matrices from the measuring bridges are obtained:

$$\begin{aligned} \mathbf{S}_{\text{exit}}^{\text{testcase1}} &= \begin{Bmatrix} 58.6075 \\ -61.2878 \end{Bmatrix} \quad \mathbf{S}_{\text{exit}}^{\text{testcase2}} = \begin{Bmatrix} 85.1673 \\ -62.5450 \end{Bmatrix} \quad \mathbf{S}_{\text{exit}}^{\text{testcase3}} = \begin{Bmatrix} 175.9310 \\ -56.3150 \end{Bmatrix} \\ \mathbf{S}_{\text{exit}}^{\text{testcase4}} &= \begin{Bmatrix} 383.9240 \\ -37.9066 \end{Bmatrix} \quad \mathbf{S}_{\text{exit}}^{\text{testcase5}} = \begin{Bmatrix} 489.9398 \\ -28.5750 \end{Bmatrix} \end{aligned}. \tag{16}$$

For such mixed signals, the following matrices of estimated original source signals Y and Q are obtained:

$$\begin{aligned} \mathbf{S}_{\text{est}}^{\text{testcase1}} &= \begin{Bmatrix} -4.074 \\ 111.055 \end{Bmatrix} \quad \mathbf{S}_{\text{est}}^{\text{testcase2}} = \begin{Bmatrix} -0.800 \\ 117.776 \end{Bmatrix} \quad \mathbf{S}_{\text{est}}^{\text{testcase3}} = \begin{Bmatrix} 12.351 \\ 123.341 \end{Bmatrix} \\ \mathbf{S}_{\text{est}}^{\text{testcase4}} &= \begin{Bmatrix} 43.520 \\ 129.609 \end{Bmatrix} \quad \mathbf{S}_{\text{est}}^{\text{testcase5}} = \begin{Bmatrix} 59.361 \\ 132.840 \end{Bmatrix} \end{aligned}. \tag{17}$$

Metrol. Meas. Syst., Vol. 30 (2023), No. 3, pp. 563–579
DOI: 10.24425/mms.2023.146424

A comparative overview of the values of parameters Y and Q, as well as the Y/Q ratio, actually set in the numerical FEM model and estimated by the inverse determination algorithm is given in Table 2.

Table 2. Comparative overview of values of parameters Y and Q, as well as the Y/Q ratio, actually set in the numerical FEM model and estimated by the inverse determination algorithm.

Test case	**Parameter Y [kN]**			**Parameter Q [kN]**			**Ratio Y/Q**		
	Set in FEM model	Estimated by IDA	Deviation	Set in FEM model	Estimated by IDA	Deviation	Set in FEM model	Estimated by IDA	Deviation
1	0	–4.074 (= 0)	0%	116	111.055	4.26%	0	–0.037 (= 0)	0%
2	0	–0.800 (= 0)	0%	119	117.776	1.03%	0	–0.007 (= 0)	0%
3	12	12.351	2.84%	123	123.341	0.28%	0.098	0.100	2.00%
4	43	43.520	1.19%	129	129.609	0.47%	0.333	0.336	0.89%
5	58	59.361	2.29%	132	132.840	0.63%	0.439	0.447	1.79%

The obtained results showed a high accuracy of the developed solution. The developed inverse determination algorithm is very efficient and provides a very reliable estimation of the unknown parameters in the wheel-rail interaction. At the parameters$Y$ and Q, the deviations between their values actually set in the numerical FEM model and the estimated values are less than 1% for Test cases 2–5, while in Test case 1 the deviation is 4.26%. As for the Y/Q ratio, the deviations between the values set in the numerical FEM model and the estimated values are even smaller *i.e.*, within 2%. When the negative value of the lateral force Y is obtained, it should be assumed that the estimated value of this parameter is equal to zero (see Table 2). This error, as well as other errors in the estimation of the parameters Y and Q, are primarily caused by small differences in strains when force Y changes the position, which is disregarded in this research.

With the aim of achieving more accurate and reliable results, additional measuring bridges could be introduced as well as more strain gauges at one radial distance, for example 8 instead of 4. This will not change the essence of the developed solution, but it will certainly increase its complexity and the cost of practical implementation. Therefore, the developed solution has great potential for additional improvement of the accuracy of inverse determination of the parameters being measured. By all means, the obtained results have validated the developed solution and have shown that it can be efficiently used for the instrumentalization of the considered wheelset BA314.

6. Conclusions

The paper presents the design of a specific type of an instrumented wheelset intended for continuous measuring of wheel-rail interaction forces Y and Q,*i.e.*the Y/Q ratio, in accordance with international regulations EN 14363 and UIC 518. The platform for developing the instrumented wheelset is the standard commercial wheelset BA314 for freight wagons with an axle-load of 25 t. Within the approach, solving all the key problems of the development of an instrumented wheelset is based on the wheel's numerical FEM model. The strain distribution on the internal and external side of the wheel disc is determined based on the results of FEM calculations in ANSYS software. Consequently, the most convenient radial distances for the installation of the strain gauges of the measuring bridges are identified. The disposition, number and way of interconnection of strain

gauges in the measuring bridges are also defined. Lastly, an algorithm for inverse determination of parameters Y and Q being measured is developed. The developed solution is validated by tests on five concrete examples using a numerical FEM model. The high accuracy of the estimation of the unknown parameters Y and Q is obtained with an error of less than 4.5%, while the error of the estimation of Y/Q ratio is less than 2%.

Accordingly, the developed solution can be efficiently used in the instrumentalization of the considered wheelset BA314. It provides high efficiency and measuring accuracy with great potential for its additional increasing. It also provides a significant reduction in the costs of development of the instrumented wheelset since key problems are solved based on the numerical FEM model instead of expensive trials on a real object. The subject of further research will be related to solving the problems of practical implementation of the developed solution such as calibration on the test rig, power supply, measuring of the wheels' angular placement, signal collection, contactless signa transmission, signals processing, improvement of the *signal-to-noise ratio* (SNR), ensuring the accuracy of installation of strain gauges, *etc.*

Acknowledgements

The authors wish to express their gratitude to the Serbian Ministry of Education, Science and Technological Development for supporting this research (contract no. 451-03-68/2022-14/200108).

References

[1] Iwnicki, S. D. (2006). *Handbook of Railway Vehicle Dynamics*. Taylor & Francis, Abingdon.

[2] Andersson, E., Berg, M., & Stichel, S. (2007). *Rail Vehicle Dynamics*. Railway Group KTH, Stockholm.

[3] European Committee for Standardization. (2018). *Railway Applications – Testing and Simulation for the Acceptance of Running Characteristics of Railway Vehicles – Running Behaviour and Stationary Tests* (Standard No. EN 14363:2016+A1:2018).

[4] UIC Railway Publications (2009) Testing and Approval of Railway Vehicles from the Point of View of their Dynamic Behaviour – Safety – Track Fatigue – Running Behaviour (4th ed.). *Railway Technical Publications*.

[5] Olson, P. E., & Johnsson, S. (1959). Seitenkräfte zwischen Rad und Schiene. *Glasers Annalen*, *83*, 153–161.

[6] Zeilhofer, M., Sühsmuth, G., & Piwenitzky, G. (1972). Ĺrmittlung der Kräfte zwischen Rad und Schiene aus den Biegedehnungen der Radsatzwelle. *Glasers Annalen*, *96*(12), 373–385.

[7] Berg, H., Gößling, G., & Zück, H. (1996). Radsatzwelle und Radscheibe – die richtige Kombination zur Messung der Kräfte zwischen Rad und Schiene. *Glasers Annalen*, *120*(2), 40–47.

[8] Allen, R. A. (1980). *A Superior Instrumented Wheelset*. Wheel/Rail Dynamics Society.

[9] Bracciali, A., Cavaliere, F., & Macherelli, M. (2014, April). Review of instrumented wheelset technology and applications. Proceedings of the Second International Conference on Railway Technology: Research, Development and Maintenance (pp. 1–16). https://doi.org/10.4203/ccp.104.167

[10] Bižić, M., & Petrović, D. (2017). Basics of experimental determination of wheel-rail contact forces by using instrumented wheelsets. *IMK-14 – Research & Development*, 23, 63–68.

[11] Diana, G., Resta, F., Braghin, F., Bocciolone, M., Di Gialleonardo, E., & Crosio, P. (2012). Metodologia di calibrazione di sale dinamometriche per la misura delle forze di contatto tra ruota e rotaia. *Ingegneria Ferroviaria*, 1, 9–21.

[12] Gialleonardo, E. D., Diana, G., Resta, F., Braghin, F., Bocciolone, M., & Crosio, P. (2011). Design of a new full scale test-rig for the calibration of instrumented wheelsets. In *Proceedings of the 9th World Congress on Railway Research – WCRR 2011*.

[13] Bracciali, A., Macherelli, M., & Bocciolini, L. (2016). Design of an Innovative Test Bench to Calibrate Instrumented Wheelsets. In *Proceedings of the Third International Conference on Railway Technology: Research, Development and Maintenance*. 243. https://doi.org/10.4203/ccp.110.243

[14] Gialleonardo, E. D., Bionda, S., Braghin, F., & Somaschini, C. (2018). Design of experiment approaches for the calibration of instrumented wheelset. In *Proceedings of 16th Mini Conference on Vehicle System Dynamics, Identification and Anomalies – VSDIA 2018*.

[15] Lin, H., Li, Q., Yuan, Y., Yu, R., & Yang, G. (2016). *Calibration Test and Correction of Instrumented Wheelset, Proceedings of Conference Advanced Science and Technology – ASTL 2016*. *121*, 476–479. https://doi.org/10.14257/astl.2016.121.86

[16] Jin, X. (2020). Evaluation and analysis approach of wheel–rail contact force measurements through a high-speed instrumented wheelset and related considerations. *Vehicle System Dynamics*, *58*(9), 1–23. https://doi.org/10.1080/00423114.2019.1612073

[17] Bagheri, V. R., Tehrani, P. H., & Younesian, D. (2017). Optimal strain gauge placement in instrumented wheelset for measuring wheel-rail contact forces. *International Journal of Precision Engineering and Manufacturing*, *18*, 1519–1527. https://doi.org/10.1007/s12541-017-0180-7

[18] Papini, S., Pugi, L., Rindi, A., Meli, E., Papini, S., & Florence, U. O. (2013). An Integrated Approach for the Optimization of Wheel-Rail Contact Force Measurement Systems. *Journal of Modern Transportation*, *21*, 95–102. https://doi.org/10.1007/s40534-013-0013-z

[19] Gomez, E., Giménez, J. G., & Alonso, A. (2011). Method for the reduction of measurement errors associated to the wheel rotation in railway dynamometric wheelsets. *Mechanical Systems and Signal Processing*, *25*(8), 3062–3077. https://doi.org/10.1016/j.ymssp.2011.05.006

[20] Cazzulani, G., Di Gialleonardo, E., Bionda, S., Bassetti, M., Crosio, P., & Braghin, F. (2017). A new approach for the evaluation and the improvement of the metrological characteristics of an instrumented wheelset for the measure of wheel–rail contact forces. *Proceedings of the Institution of Mechanical Engineers, Part F: Journal of Rail and Rapid Transit*, *231*(4), 381–393. https://doi.org/10.1177/0954409716631785

[21] Ren, Y., & Chen, J. (2019). A new method for wheel–rail contact force continuous measurement using instrumented wheelset. *Vehicle System Dynamics*, *57*(2), 269–285. https://doi.org/10.1080/00423114.2018.1460853

[22] Kanehara, H., & Fujioka, T. (2002). Measuring rail/wheel contact points of running railway vehicles. *Wear*, *253*(1-2), 275–283. https://doi.org/10.1016/S0043-1648(02)00114-X

[23] Hondo, T., Kuniyuki, S., & Doi, H. (2021). Signal processing procedure for extracting information of contact position from instrumented wheelset using with bending and shear strains for lateral force measurement. *Proceedings of the Transportation and Logistics Conference*, *2021.30:TL2-1*. https://doi.org/10.1299/jsmetld.2021.30.TL2-1

[24] Noguchi, Y. (2021). Method for Measuring Wheel/Rail Contact Positions Using Strain Gauges. *IEEJ Transactions on Industry Applications*, *141*(3), 241–248. https://doi.org/10.1541/ieejias.141.241

[25] Hondo, T., Kuniyuki, S., Tanaka, T., Suzuki, M., & Doi, H. (2021). Measurement of wheel-rail lateral force using shear strain of wheel web in railway vehicle (Comparison with a conventional bending based method under wheel rotating condition). *Transactions of the JSME*, 87(903), 21-00253. https://doi.org/10.1299/transjsme.21-00253

[26] Hondo, T., Kuniyuki, S., Tanaka, T., & Suzuki, M. (2022). Method for Measuring Lateral Force Utilizing Shear Strains inside Wheel Load Measuring Holes of Instrumented Wheelset. *Quarterly Report of Railway Technical Research Institute*, *63*(2), 139–144. https://doi.org/10.2219/rtriqr.63.2_139

[27] Hondo, T., Tanaka, T., Kuniyuki, S., & Suzuki, M. (2021, August). Cross-sensitivity characteristics of instrumented wheelset associated with longitudinal force and lateral contact position. In *International Design Engineering Technical Conferences and Computers and Information in Engineering Conference* (Vol. 85468, p. V009T09A023). American Society of Mechanical Engineers. https://doi.org/10.1115/DETC2021-67522

[28] Wei, L., Zeng, J., Wu, P., & Gao, H. (2014). Indirect method for wheel–rail force measurement and derailment evaluation. *Vehicle System Dynamics*, *52*(12), 1622-1641. https://doi.org/10.1080/00423114.2014.953180

[29] Urda, P., Muñoz, S., Aceituno, J. F., & Escalona, J. L. (2020). Wheel-rail contact force measurement using strain gauges and distance lasers on a scaled railway vehicle. *Mechanical Systems and Signal Processing*, 138, 106555. https://doi.org/10.1016/j.ymssp.2019.106555

[30] Wang, J., Li, D., Qu, S., & Zhang, D. (2021). A Nondestructive Instrumented Wheelset System for Contact Forces Measurements. *Engineering*, *13*(7), 361–371. https://doi.org/10.4236/eng.2021.137026

[31] Nong, H., & Lin, J. (2009, August). Design of loosely coupled inductive power transfer systems for instrumented wheelset. In *2009 9th International Conference on Electronic Measurement & Instruments* (pp. 1-670–1-674). IEEE. https://doi.org/10.1109/icemi.2009.5274779

[32] Ronasi, H., Johansson, H., & Larsson, F. (2014). Identification of wheel–rail contact forces based on strain measurements, an inverse scheme and a finite-element model of the wheel. *Proceedings of the Institution of Mechanical Engineers, Part F: Journal of Rail and Rapid Transit*, *228*(4), 343–354. https://doi.org/10.1177/0954409712473961

[33] Ren, Y., & Chen, J. (2009). Instrumented Wheelset Wheel/Rail Force Measurement by Blind Signal Separation. *Proceedings of the Second International Conference on Transportation Engineering – ICTE 2009*. 2502–2507. https://doi.org/10.1061/41039(345)413

[34] Ren, Y., Chen, J., & Lin, J. (2010) A Blind Signal Separation Based Measurement of the Wheel/Rail Force of an Instrumented Wheelset. *Mechanical Science and Technology for Aerospace Engineering*, 3, 289–292.

[35] Bižić, M. (2015). *Research of influential parameters in wheel-rail interaction on running stability of railway vehicles* [Doctoral dissertation, University of Kragujevac]. (in Serbian)

[36] Bižić, M. B., Petrović, D. Z., Tomić, M. C., & Djinović, Z. V. (2017). Development of method for experimental determination of wheel–rail contact forces and contact point position by using instrumented wheelset. *Measurement Science and Technology*, *28*(7), 075902. https://doi.org/10.1088/1361-6501/aa666f

[37] European Committee for Standardization. (2020). *Railway applications – Wheelsets and bogies – Wheels – Product requirements* (Standard No. EN 13262:2020).

Metrol. Meas. Syst., Vol. 30 (2023), No. 3, pp. 563–579
DOI: 10.24425/mms.2023.146424

Dr. Milan Bižić is associate professor and Vice-Dean for Science and Research at the Faculty of Mechanical and Civil Engineering in Kraljevo, University of Kragujevac, Serbia. With more than 15 years of experience, he has specialized in the field of railway engineering and experimental testing of mechanical structures. He published more than 70 scientific papers in renowned international journals and international conferences. He has participated in several domestic and two international projects. He is a permanent reviewer in the few most important world journals in the field of measurement and experimental mechanics.

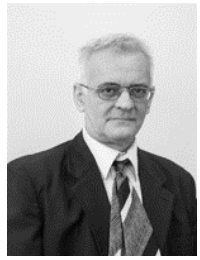

Dr. Dragan Petrović is full professor at the Faculty of Mechanical and Civil Engineering in Kraljevo, University of Kragujevac, Serbia. He is a longtime chief of the Railway Vehicles Center as well as Department for Machinery design at the same faculty. With more than 35 years of experience, he has specialized in the field of railway engineering and experimental testing of mechanical structures. He published more than 150 scientific papers in the international journals and attended both domestic and international scientific conferences. He has participated in more than 15 domestic and 4 international projects.